

Research on Efficient Numerical Calculation and Error Correction Methods for Military Precision Measurement

Jinming Zhang^{1,*}, Jun Liao¹ and Meng Li¹

¹ Aviation Maintenance NCO School, Air Force Engineering University, Xinyang, Henan, 464000, China

Corresponding authors: (e-mail: 17651777111@163.com).

Abstract Military precision measuring instruments are crucial in military fields such as weapons research and development and testing. This paper calculates the fuzzy similarity between measurement samples and fixed samples of military precision measuring instruments and measures their fuzzy similarity priority ratio based on the Hamming distance. The intercepts of similar samples are processed in order of magnitude, and the sample factor sequence values are comprehensively added to calculate the similarity between samples. The phase difference of similar samples is measured using the Fourier transform (DFT) to reduce measurement errors. The study shows that the method proposed in this paper quickly achieves a signal effective value of 6.966 when the number of frequency sampling points is 125, and the calculated uncertainty square value is less than 0.2000. In real-time error estimation, the error values of the six measuring instruments based on this method all do not exceed 1.500 mm, enabling real-time DC voltage adjustment and improving the measurement accuracy of the instruments.

Index Terms military precision measurement, fuzzy similarity, Hamming distance, Fourier transform, phase difference calculation

1. Introduction

In the military field, precision measurement technology serves as a precise tool, playing a crucial role in the design, manufacturing, maintenance, and performance enhancement of weapons [1], [2]. It is integral to every aspect of military operations, from the precise measurement of firearm components to the real-time monitoring of drone posture and various parameters, all of which rely on the robust support of precision measurement technology [3]-[5]. As military technology continues to advance, the demand for higher measurement precision has grown, driving the ongoing evolution and innovation of military precision measurement technology [6], [7].

Currently, the primary methods and technologies widely applied in military precision measurement include efficient numerical computation methods and error correction techniques [8], [9]. Numerical computation methods constitute a research field addressing the challenges of representing real numbers with finite precision in computers [10], [11]. Since the use of binary representation of real numbers in computers can cause rounding errors, error compensation has become a commonly used technical means to enhance the accuracy of military precision measurement [12]-[14]. Software error compensation methods include various algorithms such as filtering algorithms and curve fitting algorithms [15]. Filtering algorithms are divided into two types: noise-reduction filtering and smoothing filtering [16]. Noise-reduction filtering employs methods to eliminate Gaussian white noise, removing the impact of random errors on data and reducing measurement errors [17], [18]. Smoothing filtering can be used to remove outliers, making the data smoother [19]. Curve fitting algorithms analyze measurement data using mathematical models to obtain precise measurement results [20]. This method is commonly used when data follows a polynomial curve distribution, and the true values in the measurement data can be obtained using the least squares method [21], [22]. Error compensation technology has widespread application in precision measurement, enhancing the accuracy and reliability of measurement data [23]. However, it also has certain limitations, such as the possibility of introducing new errors through the compensation method itself, necessitating reasonable selection and optimization of compensation methods [24], [25]. Additionally, error compensation technology incurs higher costs, including technical, equipment, and labor expenses, requiring careful consideration based on specific circumstances [26], [27].

This paper addresses the diverse characteristics and technical requirements of military precision measuring instruments by proposing an optimized calculation method for measurement values based on fuzzy similarity theory and Fourier transform. By calculating the fuzzy similarity of the fuzzy sets of measurement values from military precision measuring instruments and combining Hamming distance analysis to determine the priority of fuzzy similarity between sample data, a fuzzy similarity matrix is constructed. Similar samples are subjected to intercept

processing and similarity ranking to determine the degree of similarity of measurement values. Fourier transform is introduced to achieve precise measurement and control of phase difference errors in similar samples, thereby enhancing the measurement accuracy and error correction capabilities of military precision measurement instruments.

II. Numerical measurement technology based on fuzzy similarity theory and Fourier transform

II. A. Characteristics and requirements of military electronic measuring instruments

The characteristics of military electronic measuring instruments can be summarized as follows:

- 1) Military electronic measuring instruments generally have a high level of technology and are high-tech products. Military electronic measuring instruments represent the highest level of electronic measuring instruments available today. Due to the advanced technology used in weapons and equipment (including electronic equipment), the military electronic measuring instruments used for measurement, testing, monitoring, control, and maintenance must also be technologically advanced. The adoption of new measurement technologies and the emergence of new products are largely driven by the updating of military equipment.
- 2) Military electronic measurement instruments come in a wide variety of categories and series, including not only electrical measurement instruments but also instruments that utilize sensors or transducers to convert non-electrical quantities into electrical quantities for measurement. Non-electrical measurement instruments also constitute a large family.
- 3) Military electronic measurement instruments generally require high precision. For example, in the measurement of parameters such as time, frequency, and distance (positioning), high precision is required.
- 4) Military electronic measurement instruments generally require a high degree of automation, fast testing speed, and simple operation, with minimal requirements for operators.
- 5) Military electronic measurement instruments generally require compact size, light weight, and low power consumption.
- 6) Military electronic measurement instruments generally require the ability to withstand harsh environmental conditions. In addition to operating in high-temperature, high-humidity, extreme cold, and high-vibration environments, they often have additional requirements such as waterproofing, salt fog resistance, chemical resistance, and nuclear radiation resistance depending on their specific applications.
- 7) Military electronic measurement instruments require strong physical survivability and functional survivability. The design for resistance to destruction is a unique feature of military electronic measurement instruments. This may also include EMP-hardened design under nuclear attack conditions.
- 8) Military electronic measurement instruments require higher reliability, with design efforts aimed at achieving "zero" faults.
- 9) Military electronic measurement instruments require higher testability, maintainability, and ease of repair.
- 10) Military electronic measurement instruments have higher standardization requirements and are required to develop toward integration and modularization, enabling multiple functions and configurations in a single device.

II. B. Fuzzy Similarity Theory

II. B. 1) Fuzzy similarity

Similarity uses a number to measure the degree of similarity between the fuzzy sets of measurement samples of two military precision measuring instruments. In fact, it is a measure of the overall information of fuzzy sets. Fuzzy similarity, on the other hand, is a measure of the degree of similarity between two fuzzy sets at a point in the domain, i.e., fuzzy similarity, which is actually a measure of the local information of two fuzzy sets.

Definition 1 If the fuzzy relation $\tilde{R} : \mu_{\tilde{R}}(x, y)$ on $X \times X$ satisfies:

Reflexivity:

$$\mu_{\tilde{R}}(x, x) = 1.0, \text{ for any } x \in X \quad (1)$$

Symmetry:

$$\mu_{\tilde{R}}(x, y) = \mu_{\tilde{R}}(y, x), \text{ for any } x, y \in X \quad (2)$$

Then \tilde{R} is called a fuzzy similarity relation. When X is a finite set, \tilde{R} is called a fuzzy similarity matrix.

Definition 2 Let $F(X)$ be the set of all fuzzy sets formed on the domain X . The mapping

$$SM : F(X) \times F(X) \rightarrow F(X), (A, B) \rightarrow SM(A, B) \quad (3)$$

For fuzzy similarity on domain X , if the following conditions are satisfied:

- 1) $\phi \subseteq SM(A, B) \subseteq X$;
- 2) When $A \neq \phi$, $SM(A, A) = X$;

3) $SM(A, B) = SM(B, A)$;

4) When $A \subseteq B \subseteq C$, we have $SM(A, C) \subseteq S(A, B) \cap S(B, C)$

At this point, for any $x \in X$, we define $SM(A(x), B(x)) \square SM(A, B)(x)$ as the similarity of the fuzzy set A, B at x .

Note 1 Let $x_0 \in X, A, B \in F(X)$, if $A(x_0) = B(x_0) \neq 0$, then $SM(A, B)(x_0) = 1.0$.

The following are several formulas for fuzzy similarity, all of which satisfy the conditions of Definition 2:

$$SM(A, B)(x) = \begin{cases} \frac{A(x) \wedge B(x)}{A(x) \vee B(x)}, & A(x) \vee B(x) > 0.00 \\ 0.00, & A(x) \vee B(x) = 0.00 \end{cases} \quad (4)$$

$$SM(A, B)(x) = \begin{cases} 1.00 - \frac{A(x) - B(x)}{A(x) \vee B(x)}, & A(x) \vee B(x) > 0.00 \\ 0.00, & A(x) \vee B(x) = 0.00 \end{cases} \quad (5)$$

$$SM(A, B)(x) = (A \rightarrow B)(x) \wedge (B \rightarrow A)(x) \quad (6)$$

The operator contained therein is R_0 implication, that is:

$$(A \rightarrow B)(x) = \begin{cases} 1, & A(x) \leq B(x) \\ A(x) \vee B(x), & A(x) > B(x) \end{cases} \quad (7)$$

II. B. 2) Fuzzy similarity priority ratio

Similarity priority ratio: A measure used to determine which of two objects is more similar to a third object, from which the one with a higher degree of similarity to the fixed sample is selected.

Assuming that samples x_i and x_j are compared with the fixed sample x_k , their similarity priority ratio r_{ij} must satisfy the following requirements:

- 1) If r_{ij} is in the range $[0.50, 1.00]$, then x_i is preferred over x_j ;
- 2) If r_{ij} is in the range $[0.00, 0.50]$, then x_j is preferred over x_i ;
- 3) In extreme cases, there are three possibilities: if $r_{ij} = 1.00$, then x_i is clearly preferred over x_j ; If $r_{ij} = 0.00$, it indicates that x_j is clearly preferred over x_i ; If $r_{ij} = 0.50$, the preference between x_i and x_j cannot be determined.

In fuzzy similarity priority ratio analysis, the Hamming distance is generally used as the measure of r_{ij} in the similarity priority ratio. When comparing samples x_i and x_j with a fixed sample x_k , the Hamming distance can be defined as:

$$r_{ij} = \frac{|x_k - x_j|}{|x_k - x_i| + |x_k - x_j|}, r_{ji} = 1 - r_{ij} \quad (8)$$

Next, for a given sample set $\bar{X} = \{x_1, x_2, \dots, x_n\}$ and a fixed sample x_k , compare any x_i , x_j , and x_k , i.e., calculate the similarity priority ratio between each pair of samples to obtain the fuzzy correlation matrix:

$$\tilde{R} = (r_{ij}) \begin{cases} r_{ij} \in [0.00, 1.00] \\ i, j = 1, 2, \dots, n \end{cases} \quad (9)$$

After establishing the fuzzy similarity matrix, similar samples are selected based on the λ level cutoff. Specifically, in the similarity matrix, λ values are selected in descending order, and the samples in the row that first reaches a value where all elements except the main diagonal are 1.00 are considered the most similar. Then, the corresponding row and column of the matrix are deleted, and the λ level value is lowered to continue the search. This process is repeated until the truncation is complete.

Generally, if each sample has m factors, then there is a fuzzy similarity matrix for each factor. Therefore, each factor of each sample will produce a serial number value reflecting the degree of similarity. Finally, the serial number values of each factor of each sample are added together, and the result is a comprehensive reflection of the similarity between the sample and the fixed sample.

The smaller the numerical value of a sample, the more similar it is to the fixed sample. However, strictly speaking, the influence of each factor on the sample is not the same, so it is necessary to assign certain weights to each factor. This will yield results that better reflect the actual situation. Therefore, each factor can be weighted to achieve better analytical results.

II. C. Phase difference measurement principle based on DFT

For a discrete sequence $x(n)$ of length N , its discrete Fourier transform is:

$$X(k) = \sum_{n=0}^{N-1} x(n)e^{j2\pi kn/N}, 0.00 \leq k \leq N-1.00 \quad (10)$$

In the formula: $X(k)$ — a complex variable function related to the frequency index k .
It can be expressed in rectangular coordinates and polar coordinates as follows:

$$X(k) = X_{re}(k) + jX_{im}(k) = |X(k)|e^{j\theta(k)} \quad (11)$$

In the formula:

$$\begin{aligned} |X(k)| &= \sqrt{X_{re}(k)^2 + X_{im}(k)^2} \\ \theta(k) &= \arctan \frac{X_{im}(k)}{X_{re}(k)} \end{aligned} \quad (12)$$

Using the real and imaginary parts after the DFT transformation, the phase angle of the signal can be calculated.
For a specific sine wave signal $x(t)$, its mathematical expression can be represented as:

$$x(t) = A \cos(\omega t + \varphi) \quad (13)$$

In the equation:

A — signal amplitude;

$\omega = 2\pi f_0$ — signal angular frequency;

$\omega t + \varphi$ — signal phase;

φ — initial phase angle of the signal (also known as phase angle).

For two sinusoidal signals of the same frequency, the phase difference can be obtained by subtracting the phase angles of the two signals, i.e.:

$$\Delta\varphi = (\omega t + \varphi_1) - (\omega t + \varphi_2) = \varphi_1 - \varphi_2 \quad (14)$$

In the formula: φ_1 and φ_2 are the phase angles of two measured sine signals with the same frequency.

When the signal $x(t)$ is sampled at a sampling frequency f_s , the discrete sequence with a sampling length of N is:

$$x(n) = A \cos(2\pi qn/N + \varphi), 0.00 \leq n \leq N-1.00 \quad (15)$$

In the formula: $q = Nf_0 / f_s$ When q is an integer, the sampling process is integer-period sampling, and there is no spectrum leakage; when q is not an integer, the sampling process is non-integer-period sampling, and spectrum leakage occurs.

Performing a discrete Fourier transform on the discrete sequence $x(n)$ obtained by sampling $x(t)$ yields the signal spectrum, which can be expressed as:

$$\begin{aligned} X(k) &= \sum_{n=0}^{N-1} x(n)e^{-j2\pi kn/N} \\ &= \sum_{n=0}^{N-1} A \frac{(e^{j2\pi qn/N + j\varphi} + e^{-j2\pi qn/N - j\varphi})}{2} e^{-j2\pi kn/N} \\ &= \frac{Ae^{j\varphi}}{2} \sum_{n=0}^{N-1} e^{j2\pi(q-k)n/N} + \frac{Ae^{-j\varphi}}{2} \sum_{n=0}^{N-1} e^{j2\pi(q+k)n/N} \\ &0.00 \leq k \leq N-1.00 \end{aligned} \quad (16)$$

When q is an integer, based on the characteristics of the complex exponential sequence, we know that when $k = q$, $X(k) = NAe^{j\varphi}/2$, when $k = N - q$, $X(k) = NAe^{-j\varphi}/2$, and when k is any other value, $X(k) = 0$. Therefore, by searching for the spectrum with the maximum amplitude within the range $0 \leq k \leq N/2$, the phase angle of the signal $x(t)$ can be accurately measured. When q is not an integer, if the phase angle is measured by searching for the spectrum with the maximum amplitude in the same way, the effect of frequency leakage will inevitably introduce measurement errors.

III. Simulation experiment based on fuzzy similarity theory and Fourier transform

III. A. Establishment of sample fuzzy sets

III. A. 1) Sample Measurement and Preprocessing

Based on the primary performance requirements of military precision measuring instruments, the key parameter “horizontal target positioning repeatability” was selected to establish a sample fuzzy set. The measurement method employed direct measurement. Ten measurement groups were selected, with each group undergoing four repeated measurements. Considering that outliers may exist in the measurements and need to be excluded (if no outliers are

present, all data are used), measurements are conducted once every month, with each group consisting of 4 measurements, totaling 12 groups. Table 1 summarizes the process parameters for horizontal target positioning repeatability. Among the 12 sets of measurement sample data, the average values of the 4 measurements in the 6th and 8th groups reached 2.04" and 2.57", respectively, which differed significantly from the average values of other groups. These were attributed to measurement errors, so the measurement data from the 6th and 8th groups were excluded. The remaining 10 groups of data were renumbered from 1 to 10 and used as the sample data for this study.

Table 1: Sample parameters for the repeatability of horizontal target positioning

Number of groups	Number of times				\bar{x}_j
	1	2	3	4	
1	0.26"	0.76"	0.16"	0.35"	0.39"
2	0.87"	0.81"	1.32"	1.41"	1.08"
3	0.95"	1.65"	0.85"	0.72"	1.02"
4	1.27"	1.43"	1.19"	1.26"	1.29"
5	1.98"	1.75"	1.89"	1.42"	1.76"
6	2.04"	1.62"	2.12"	2.27"	2.04"
7	1.35"	1.95"	1.97"	1.53"	1.72"
8	2.61"	2.94"	1.95"	2.76"	2.57"
9	0.96"	0.78"	0.84"	0.95"	0.89"
10	0.84"	0.87"	0.89"	0.85"	0.86"
11	0.72"	0.63"	0.67"	0.75"	0.69"
12	0.26"	0.76"	0.16"	0.35"	0.39"

III. A. 2) Checking measurement results

Conduct verification of the measurement sample data, with each group undergoing 5 verification checks. Within the two calibration intervals, one group is verified every month. Table 2 presents the measurement results data. Here, \bar{x}_j represents the measurement average, and s_j represents the experimental standard deviation of the measurement values. Figure 1 illustrates the control status of the verification average values during the measurement process. The average values of the 10 verification measurement results are 0.38", 1.06", 1.02", 1.27", 1.76", 1.71", 0.88", 0.85", 0.67", and 0.37", respectively, all within the control limits of 2.76" and -0.76". The measurement standard state is under control. This demonstrates that using military-grade precision measurement instruments for numerical measurements can yield valid sample data within the control limits.

Table 2: The measurement result data after technical processing

Number of groups	Measurement result						s_j
	1	2	3	4	5	\bar{x}_j	
1	0.36"	0.37"	0.39"	0.38"	0.38"	0.38"	0.010"
2	1.06"	1.06"	1.05"	1.07"	1.07"	1.06"	0.014"
3	1.00"	1.01"	1.03"	1.04"	1.01"	1.02"	0.014"
4	1.26"	1.26"	1.27"	1.27"	1.28"	1.27"	0.008"
5	1.77"	1.75"	1.77"	1.77"	1.75"	1.76"	0.015"
6	1.71"	1.70"	1.71"	1.71"	1.72"	1.71"	0.008"
7	0.88"	0.88"	0.87"	0.88"	0.87"	0.88"	0.005"
8	0.85"	0.85"	0.87"	0.85"	0.84"	0.85"	0.010"
9	0.67"	0.68"	0.66"	0.68"	0.68"	0.67"	0.008"
10	0.37"	0.37"	0.36"	0.37"	0.38"	0.37"	0.008"

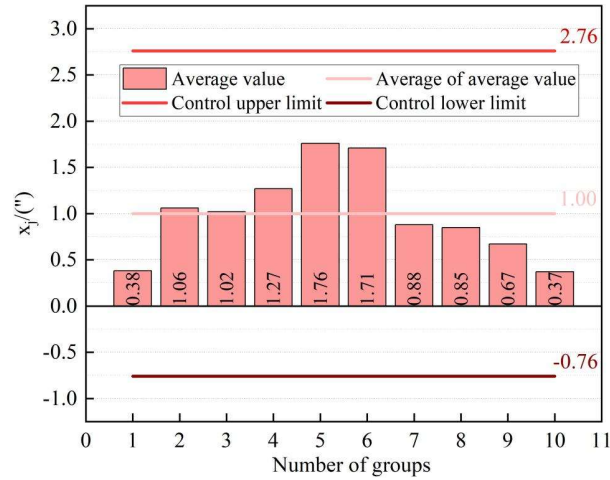


Figure 1: Control of verification average value during the measurement process

III. B. Simulation Experiment

III. B. 1) Simulation of algorithm results

Multiple military electronic measurement instruments were selected as test devices for simulation experiments. The MATLAB/Simulink simulation software was used to perform signal processing of similar samples using the Fourier transform. The signal processing effects of the traditional Fourier transform and the Fourier transform technology combined with fuzzy similarity theory were compared. Figure 2 shows the specific process of how the effective value of the signal $x(t)$ changes with the number of sampling points N as the frequency increases. From the comparison of simulation results between the two algorithms, the signal effective value of the Fourier transform technique combined with fuzzy similarity theory reaches a stable 6.966 when N equals 125, while the signal effective value of the traditional Fourier transform technique requires N to reach 848 to achieve a stable 6.933. The method proposed in this paper can obtain higher signal effective values more quickly, with faster measurement calculations and error correction speeds.

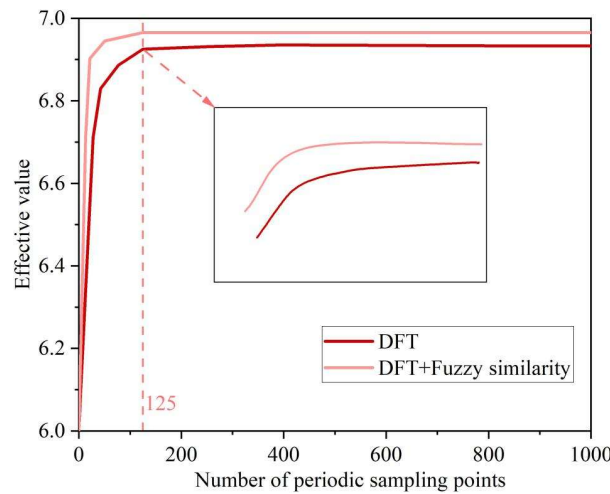


Figure 2: Simulation results of two algorithms

III. B. 2) Calculation of determinacy rating

The voltage reading V_r of military-grade electronic precision measurement instruments must be evaluated using the Class A measurement uncertainty component evaluation method. Sources of uncertainty include measurement system instability and the repeatability of operator actions. Since the testing system for military-grade electronic precision measurement instruments is a closed-loop automatic testing system, all tested instruments must maintain an injected interference level of 1.00V. Therefore, the sources of Class A measurement uncertainty also include the uncertainty of the tested instruments.

A-class standard uncertainty calculations were performed on 10 sets of measurement sample data after Fourier signal processing. Table 3 shows the A-class evaluation calculation results for the measurement instrument

readings after Fourier transformation. Only the uncertainty square of the 7th set of measurement sample data exceeded 1, while the uncertainty squares of the remaining 9 sets of measurement data were all less than 0.2000, indicating low uncertainty.

Table 3: Class A assessment results of the readings of measuring instruments

Measurement group	Measured value R(dBuV)	$v = R - \bar{R}$	v^2
1	115.6742	0.1707	0.0291
2	115.1263	-0.3772	0.1424
3	115.2701	-0.2334	0.0545
4	115.1290	-0.3745	0.1403
5	115.1317	-0.3718	0.1384
6	115.1232	-0.3803	0.1444
7	110.1903	-5.3132	28.2290
8	115.1190	-0.3845	0.1480
9	115.1467	-0.3568	0.1274
10	115.2946	-0.2089	0.0438
Sum	1155.0352	-	28.9550
VLAW	115.5035	-	-

III. B. 3) Real-time error estimation performance test

With the support of a simulation platform, a real-time estimation test of measurement errors in military electronic measuring instruments was conducted based on fuzzy similarity theory and Fourier transform. The prepared electronic instrument test subjects and their measurement sample data were input into the corresponding running program to obtain the estimated results of measurement errors in military electronic measuring instruments at any given time. Figure 3 shows the changes in the measurement process of military electronic measuring instruments. Figure 4 shows the real-time estimation results of measurement errors in instruments based on different technologies. Within the 0-10s time range, the distance between the military electronic measurement instrument and the target varies between 0-34m, while the instrument's transmission power fluctuates within the 0-45W range. The actual measurement values of the six military electronic instruments using this method are 23.756, 34.870, 18.830, 39.994, 23.993, 33.767 mm, with errors relative to the actual values of 0.492, 0.492, 1.006, 0.611, 0.255, and 1.341 mm, respectively. All error values are less than 1.500 mm and also smaller than the measurement errors of instruments supported by the other two technologies, enabling real-time determination of the specific measurement conditions within a one-second time unit.

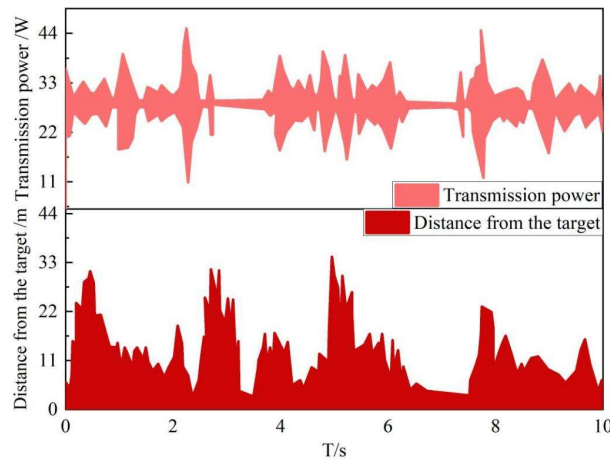


Figure 3: The changes in the instrument measurement process

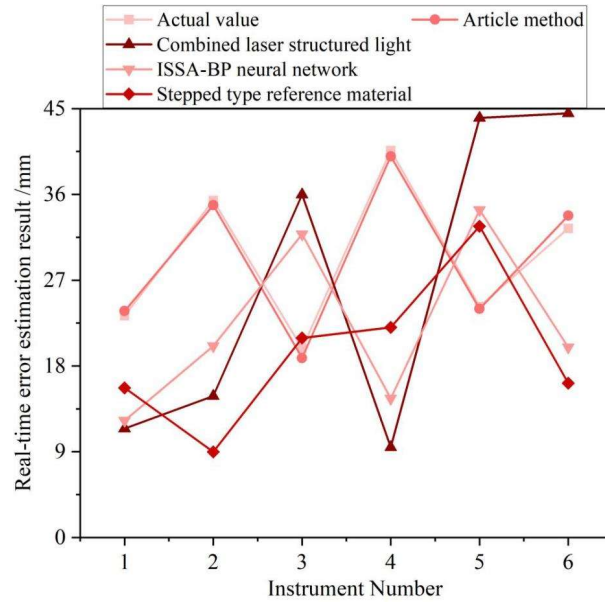


Figure 4: Real-time error estimation performance test results

III. B. 4) Analysis of DC voltage signals in simulation input

Based on the real-time error estimation results, the input DC voltage is adjusted to enhance the accuracy of real-time measurements in military electronic measuring instruments. Taking the DC voltage input conditions within a 60ms period as an example, the real-time adjustment effects based on the error estimation results are analyzed. Figure 5 shows the simulated DC voltage waveform within 60 ms. Within the 0-60 ms measurement time, based on the real-time error estimation results, the input DC voltage can be adjusted at the millisecond level, with a voltage adjustment range of 452.5-457.5 kV, and can achieve rapid multiple adjustments, enabling military electronic measurement instruments to achieve higher measurement accuracy.

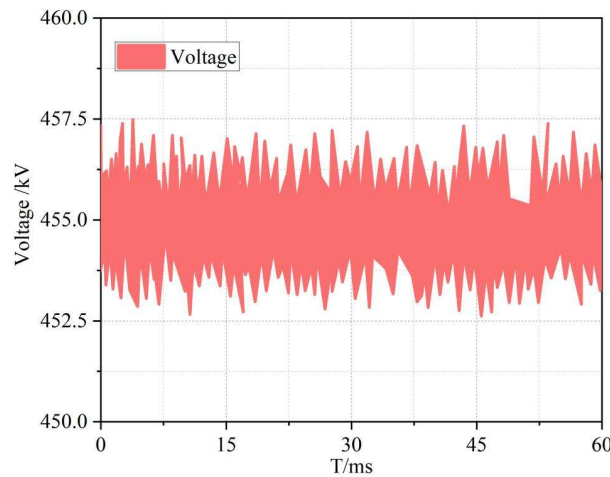


Figure 5: Simulate the input DC voltage waveform

IV. Conclusion

This paper introduces fuzzy similarity theory and Fourier transform techniques to perform real-time signal processing and error calculation for measurement signals from military precision measuring instruments, thereby improving measurement efficiency and accuracy. Through simulation experiments, the instrument based on the method proposed in this paper achieves an effective signal value of 6.966 at $N=125$, outperforming traditional Fourier methods. The mean square calculation uncertainty for nine sets of sample data is less than 0.2000, indicating high calculation precision. The measurement errors between the measured values and actual values for six measurement instruments were 0.492, 0.492, 1.006, 0.611, 0.255, and 1.341 mm, all below 1.500 mm. Based on the error estimation results, millisecond-level and kilowatt-level adjustments to the DC voltage input can be

achieved, ensuring the instrument maintains high measurement accuracy. In the future, multi-instrument collaborative measurement technology can be explored to meet the high-precision real-time measurement requirements of large-scale measurement sites.

References

- [1] Mansoor, P. R. (2019). The Precision-Information Revolution in Military Affairs and The Limits of Technology. In *Technology, Violence, and War* (pp. 333-354). Brill.
- [2] Moon, T. S., & Ryu, K. (2012). Precise measurement device for angular deviation of canopy transparency in fighter aircraft. *International Journal of Precision Engineering and Manufacturing*, 13, 347-356.
- [3] Zivkovic, A. B., Hristov, N. P., Jerković, D. D., Bogdanović, B. S., & Milutinović, J. M. (2019, October). Automatic measurement of precision and accuracy from the hit pattern of small arms using electronic target system. In *IOP conference series: materials science and engineering* (Vol. 659, No. 1, p. 012015). IOP Publishing.
- [4] Buga, A., Decker, D. D., Robinson, B. T., Crabtree, C. D., Stoner, J. T., Arce, L. F., ... & Volek, J. S. (2024). The VirTra V-100 Is a Test-Retest Reliable Shooting Simulator for Measuring Accuracy/Precision, Decision-Making, and Reaction Time in Civilians, Police/SWAT, and Military Personnel. *The Journal of Strength & Conditioning Research*, 38(10), 1714-1723.
- [5] Lindsey, B., Hanley, C., Reider, L., Snyder, S., Zhou, Y., Bell, E., ... & Bar-Kochba, E. (2025). Accuracy of heart rate measured by military-grade wearable ECG monitor compared with reference and commercial monitors. *BMJ Mil Health*, 171(2), 144-149.
- [6] Kim, M. S., Yu, S. B., & Lee, K. S. (2014). Development of a high-precision calibration method for inertial measurement unit. *International journal of precision engineering and manufacturing*, 15, 567-575.
- [7] Kott, A., & Perconti, P. (2018). Long-term forecasts of military technologies for a 20–30 year horizon: An empirical assessment of accuracy. *Technological Forecasting and Social Change*, 137, 272-279.
- [8] Qu, X., Wang, Y., Fu, G. Y., & Ma, G. W. (2015). Efficiency and accuracy verification of the explicit numerical manifold method for dynamic problems. *Rock Mechanics and Rock Engineering*, 48, 1131-1142.
- [9] Hu, C. A., Li, W., Zhou, Y., Du, W., Peng, Y., & Li, J. (2021, April). Application of the precision industrial measurement technology in geometric measurement. In *Journal of Physics: Conference Series* (Vol. 1885, No. 2, p. 022021). IOP Publishing.
- [10] Learning, L. (2021). Accuracy, Precision, and Significant Figures. *Fundamentals of Heat, Light & Sound*.
- [11] Ji, J., Shi, B., & Deng, H. (2024). Numerical calculation method. In *Vibration and Heat Transfer of Elastic Tube Bundles in Heat Exchangers: A Numerical Study* (pp. 35-49). Singapore: Springer Nature Singapore.
- [12] Zhao, J., Ou, W., Cai, N., Wu, Z., & Wang, H. (2024). Measurement error analysis and compensation for optical encoders: A Review. *IEEE Transactions on Instrumentation and Measurement*.
- [13] Liu, J., Chen, Q., Wang, J., Sun, S., Zhang, X., Du, J., ... & Yan, W. (2023). Geometric error modeling and compensation for high precision composite optical measurement systems. *Optics Express*, 31(25), 42015-42035.
- [14] Wang, S. M., Lee, C. Y., Gunawan, H., & Yeh, C. C. (2022). On-line error-matching measurement and compensation method for a precision machining production line. *International Journal of Precision Engineering and Manufacturing-Green Technology*, 9(2), 493-505.
- [15] Bepal'ko, V., Litvinenko, A., Stepanovs, V., Kurtenoks, V., Smetska, V., & Lapkovskis, V. (2024). Compensation of Accuracy Error for Time Interval Measurements. *Latvian Journal of Physics and Technical Sciences*, 61(1), 43-51.
- [16] Zhang, J., Zou, L., Zhang, X., Wang, Z., & Wang, W. (2025). An error compensation method for on-machine measuring blade with industrial robot. *Measurement*, 242, 116039.
- [17] Liu, H., Yang, R., Wang, P., Chen, J., Xiang, H., & Chen, G. (2020). Measurement point selection and compensation of geometric error of NC machine tools. *The International Journal of Advanced Manufacturing Technology*, 108, 3537-3546.
- [18] Li, W., Wu, J., Li, D., Tian, Y., & Tian, J. (2019). Telecentricity based measurement error compensation in the bilateral telecentric system. *Measurement*, 147, 106822.
- [19] Ge, G., Du, Z., Feng, X., & Yang, J. (2020). An integrated error compensation method based on on-machine measurement for thin web parts machining. *Precision Engineering*, 63, 206-213.
- [20] Gavin, H. P. (2019). The Levenberg-Marquardt algorithm for nonlinear least squares curve-fitting problems. *Department of Civil and Environmental Engineering Duke University August*, 3, 1-23.
- [21] Balaji, C., & Balaji, C. (2021). Curve fitting. *Thermal System Design and Optimization*, 69-128.
- [22] Hu, C., Wang, Z., Zhu, Y., & Zhang, M. (2018). Accurate three-dimensional contouring error estimation and compensation scheme with zero-phase filter. *International Journal of Machine Tools and Manufacture*, 128, 33-40.
- [23] Chiu, W. H., Huang, Y. H., & Lin, T. H. (2010). A dynamic phase error compensation technique for fast-locking phase-locked loops. *IEEE Journal of Solid-State Circuits*, 45(6), 1137-1149.
- [24] Geng, Z., Tong, Z., & Jiang, X. (2021). Review of geometric error measurement and compensation techniques of ultra-precision machine tools. *Light: Advanced Manufacturing*, 2(2), 211-227.
- [25] Ghimire, S., Deo, R. C., Casillas-Pérez, D., & Salcedo-Sanz, S. (2024). Two-step deep learning framework with error compensation technique for short-term, half-hourly electricity price forecasting. *Applied Energy*, 353, 122059.
- [26] Lan, L., Hua, F., Fang, F., & Jiang, W. (2024). Active Compensation Technology for the Target Measurement Error of Two-Axis Electro-Optical Measurement Equipment. *Sensors*, 24(4), 1133.
- [27] Li, R., Ding, N., Zhao, Y., & Liu, H. (2023). Real-time trajectory position error compensation technology of industrial robot. *Measurement*, 208, 112418.